

# Building Real-time Awareness of Out-of-distribution in Trajectory Prediction for Autonomous Vehicles

TONGFEI GUO, Northeastern University, USA

TAPOSH BANERJEE, University of Pittsburgh, USA

RUI LIU, Kent State University, USA

LILI SU, Northeastern University, USA

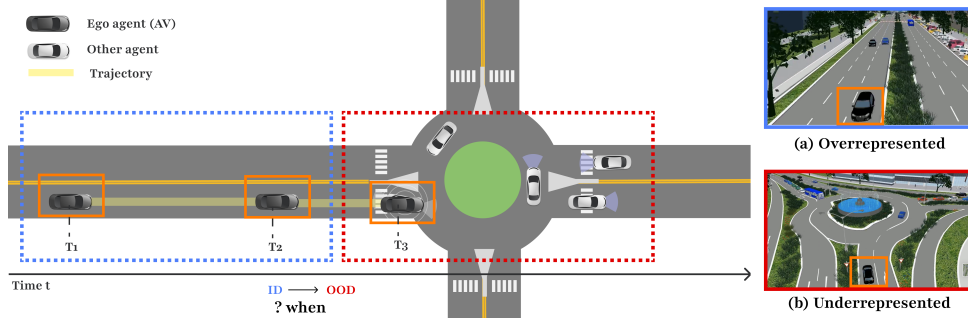


Fig. 1. An AV enters from overrepresented straight lanes (ID scene) to an underrepresented complex intersection (OOD scene) at time  $t$ . As the AV is not familiar with the intersection, it may make wrong trajectory predictions on neighboring vehicles, resulting in collisions. If we can infer the time  $t$  that AV enters OOD scenes, we can pass back the controls to human drivers in time.

Accurate trajectory prediction is essential for the safe operation of autonomous vehicles in real-world environments. Even well-trained machine learning models may produce unreliable predictions due to discrepancies between training data and real-world conditions encountered during inference. In particular, the training dataset tends to overrepresent common scenes (e.g., straight lanes) while underrepresenting less frequent ones (e.g., traffic circles). In addition, it often overlooks unpredictable real-world events such as sudden braking or falling objects. To ensure safety, it is critical to detect in real-time when a model's predictions become unreliable. Leveraging the intuition that in-distribution (ID) scenes exhibit error patterns similar to training data, while out-of-distribution (OOD) scenes do not, we introduce a principled, real-time approach for OOD detection by framing it as a change-point detection problem. We address the challenging settings where the OOD scenes are deceptive, meaning that they are not easily detectable by human intuitions. Our lightweight solutions can handle the occurrence of OOD at any time during trajectory prediction inference. Experimental results on multiple real-world datasets using a benchmark trajectory prediction model demonstrate the effectiveness of our methods.

CCS Concepts: • **Computing methodologies** → **Sequential decision making** ; • **Mathematics of computing** → **Probability and statistics**.

Authors' Contact Information: Tongfei Guo, guo.t@northeastern.edu, Northeastern University, Boston, Massachusetts, USA; Taposh Banerjee, University of Pittsburgh, Pittsburgh, USA, taposh.banerjee@pitt.edu; Rui Liu, Kent State University, Kent, USA, rliu11@kent.edu; Lili Su, Northeastern University, Boston, Massachusetts, USA, lsu@northeastern.edu.

Permission to make digital or hard copies of all or part of this work for personal or classroom use is granted without fee provided that copies are not made or distributed for profit or commercial advantage and that copies bear this notice and the full citation on the first page. Copyrights for components of this work owned by others than the author(s) must be honored. Abstracting with credit is permitted. To copy otherwise, or republish, to post on servers or to redistribute to lists, requires prior specific permission and/or a fee. Request permissions from permissions@acm.org.

© 2025 Copyright held by the owner/author(s). Publication rights licensed to ACM.

Manuscript submitted to ACM

Manuscript submitted to ACM

Additional Key Words and Phrases: autonomous vehicles, trajectory prediction, machine learning, out-of-distribution detection

#### ACM Reference Format:

Tongfei Guo, Taposh Banerjee, Rui Liu, and Lili Su. 2025. Building Real-time Awareness of Out-of-distribution in Trajectory Prediction for Autonomous Vehicles. 1, 1 (April 2025), 24 pages. <https://doi.org/10.1145/nnnnnnnn.nnnnnnnn>

## 1 INTRODUCTION

AI technologies are the backbone of modern autonomous vehicles (AVs), and are reshaping transportation systems. Accurate trajectory prediction is essential for the safe operation of autonomous vehicles in real-world environments. However, even well-trained machine learning (ML) models may produce unreliable predictions due to discrepancies between training data and real-world conditions encountered during inference. Specifically, many public datasets overrepresent certain driving scenes (e.g. straight lanes and high-ways) while significantly underrepresenting others (e.g. complex traffic circles or intersections), as illustrated in Fig. 1. Moreover, real-world environments suffer a wide range of uncertainties such as sudden braking by nearby vehicles, large objects falling from other vehicles, or other deceptive yet life-threatening distribution shifts [14, 63, 76]. As a consequence, an AV may unexpectedly run into driving scenarios that are poorly represented by the training data, which we refer to as *out-of-distribution (OOD) data*. To ensure safety, it is critical to detect in real-time when a ML model’s trajectory predictions become unreliable, allowing control to be seamlessly transferred back to human drivers.

Prior works focus on improving trajectory prediction reliability through anomaly detection [70] and uncertainty estimation [65]. However, these methods typically rely on the assumption that the training data fully represent real-world scenarios. Anomaly detection methods, such as RNN-based models, require fully representative training data to learn sequential dependencies and detect unusual trajectory patterns, such as sudden direction changes or irregular speeds [59]. Similarly, uncertainty estimation methods like variational autoencoders (VAEs) rely on comprehensive training data to model reliable distributions and flag anomalies via reconstruction errors [21]. Insufficient data coverage hinders their ability to quantify uncertainty in novel situations, degrading performance.

Some OOD scenes are easy to detect, such as sudden acceleration or rapid lane changes across multiple lanes. In this paper, we focus on a more challenging and practically relevant setting where OOD scenes are **deceptive**—meaning they are not easily identifiable by human intuition. Specifically, we examine subtle changes in the driving behavior of neighboring vehicles that maintain motion patterns within expected variations, making them difficult to distinguish from normal behavior. Building on the intuition that in-distribution (ID) driving scenes exhibit prediction error distributions similar to those observed during training, while OOD scenes deviate from this pattern, we closely monitor the sequence of prediction errors. We frame the trajectory prediction OOD awareness problem as a quickest change-point detection (QCD) problem. Drawing on well-established techniques of sequential analysis, we develop principled and lightweight OOD detection methods that offer formally assured performance in the trade-off between detection delay and false alarm.

**Contributions.** We are the first to apply QCD methods to detect OOD on multiple real-world trajectory prediction datasets. Our solutions are lightweight (monitoring a scalar variable of the prediction errors only) and can handle the occurrence of OOD at any time during inference. We summarize our main contributions as follows:

- We observe that pre- and post-change trajectory prediction errors are well-modeled as Gaussian Mixture Models, forming the basis of our OOD detection framework.

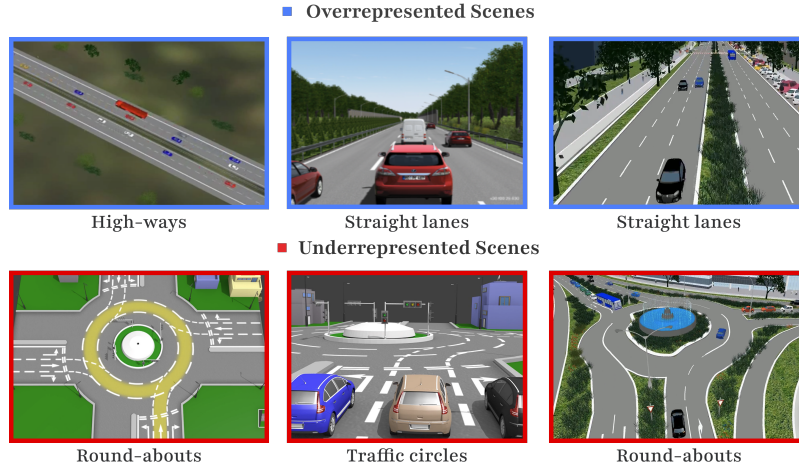


Fig. 2. Illustration of overrepresented and underrepresented scenes for the deployed ML models. Images from PTV Vissim simulation.

- We adapt the CUSUM algorithm for OOD detection, achieving 95% faster detection with minimal false alarms compared to classical sequential methods.
- We test robustness across varying levels of distribution knowledge (complete, partial, unknown), showing our method remains the most effective in challenging scenarios.

## 2 RELATED WORK

### 2.1 Trajectory Prediction

Safe autonomous driving in dynamic environments requires predicting future states of nearby traffic agents, particularly surrounding vehicles. Trajectory prediction methods for AVs are categorized into four types: physics-based, classic machine learning, deep learning, and reinforcement learning approaches. Physics-based methods use kinematic [1, 41] or dynamic [25, 37, 51] models. These approaches are simple and computationally efficient but struggle with long-term predictions in static environments, as they ignore complex interactions and environmental factors. Classic machine learning methods, such as Gaussian Processes [74], Hidden Markov Models [10], Dynamic Bayesian Networks [35], and Gaussian Mixture Models [45], improve prediction accuracy and extend time horizons. However, their reliance on predefined maneuvers limits adaptability to diverse driving scenarios. Deep learning architectures—including RNNs [24], CNNs [8, 52], and GNNs [31]—represent the state-of-the-art. These models excel in complex environments and long-term predictions by integrating interaction patterns and map data. Yet, they demand large training datasets and face trade-offs between computational efficiency and real-time performance. Reinforcement learning methods, such as inverse reinforcement learning [16, 57] and imitation learning [6, 53], mimic human decision-making to generate accurate long-horizon trajectories. However, they suffer from high computational costs and lengthy training processes. Existing literature often assumes training data comprehensively covers all driving scenarios, a premise rarely valid in practice [14]. Consequently, while current models perform well in ID scenes, their reliability degrades significantly in OOD scenarios. This limitation underscores the critical need for robust trajectory prediction to ensure AV safety in unseen dynamic environments.

## 2.2 Out-of-Distribution Detection

OOD detection is critical for ensuring the reliability of ML models in open-world settings, where they frequently encounter scenarios not represented in the training data. OOD data can emerge from a variety of sources, including environmental variability, unusual interactions, and intentional or rare events [33]. For instance, environmental factors such as unexpected weather conditions (*e.g.*, heavy rain, fog, or snow), abrupt lighting changes (*e.g.*, transitions from daylight to nighttime), or unfamiliar road types (*e.g.*, unpaved or construction zones) can introduce OOD scenes that were not accounted for during model training. Additionally, unpredictable behaviors from other road users—such as sudden stops, erratic lane changes, or jaywalking pedestrians—can further exacerbate the occurrence of OOD data. When trajectory prediction models encounter OOD data, their performance often degrades, leading to unreliable or unsafe predictions that can compromise the safety and efficacy of AV systems [12, 32]. Traditional OOD detection methods often rely on scoring functions that estimate the likelihood of a sample belonging to the training distribution, either through output-based approaches like maximum softmax probability [18] and energy scores [39], or representation-based methods that perform density estimation in lower-dimensional latent spaces, often modeled as Gaussian [30, 56] or using non-parametric techniques [60]. Despite their utility, these methods face challenges in high-dimensional domains like trajectory prediction. Density estimation becomes computationally intensive and struggles with real-time scalability, a critical requirement for low-latency AV systems. Additionally, no single approach consistently outperforms others across benchmarks [62], highlighting generalization limitations. Motivated by these computational and performance constraints, we propose exploring efficient, domain-specific techniques—particularly sequential analysis—to enable real-time OOD detection in dynamic environments.

## 2.3 Change-point Detection

Change-point detection identifies abrupt shifts in time series data and has been extensively studied in statistics, signal processing, and machine learning, with applications in finance, bioinformatics, climatology, and network monitoring [22, 42, 55, 67, 75]. The objective was to detect a shift in the mean of independent and identically distributed (iid) Gaussian variables for the purpose of industrial quality control. A prominent branch of change point detection is quickest change detection (QCD), which focuses on detecting distributional shifts as rapidly as possible while controlling false alarms [71]. QCD is typically formulated under Bayesian and non-Bayesian frameworks. In the Bayesian setting, where the change point is treated as a random variable with a known prior, the Shiryaev test provides an optimal solution by declaring a change when the posterior probability exceeds a threshold [58, 69]. Recent findings on QCD within the Bayesian framework are available in [2, 17, 19, 66]. In the non-Bayesian framework, the change point is unknown, and the objective is to minimize the worst-case detection delay, leading to the minimax-optimal Cumulative Sum (CUSUM) algorithm [40, 47, 49]. CUSUM sequentially accumulates deviations from an expected baseline and triggers an alarm when a predefined threshold is crossed, making it first-order asymptotically optimal [47, 71]. We believe that CUSUM is naturally well-suited for OOD detection due to its ability to identify deviations in real-time prediction errors. Its effectiveness has led to its widespread adoption in time-sensitive domains, as evidenced by prior research [7, 48, 68].



Table 1. Main notations used throughout the paper.

Notation	Description
$\mathcal{D}$	Dataset
$N$	Number of driving scenes
$S_j$	A single driving scene described by the triple $S_j = (\mathcal{X}_j, \mathcal{Y}_j, \mathcal{M})$
$\mathcal{X}_j$	Collection of observed trajectories in scene $S_j$ , $\mathcal{X}_j = \{x_j^1, \dots, x_j^{m_j}\}$
$\mathcal{Y}_j$	Collection of future trajectories to be predicted based on $\mathcal{X}_j$ , $\mathcal{Y}_j = \{y_j^1, \dots, y_j^{m_j}\}$
$\mathcal{M}$	Map information; if unavailable, $\mathcal{M} = \emptyset$
$m_j$	Number of agents (vehicles, pedestrians, etc.) in scene $S_j$
$L_I$	Number of time frames in the history trajectory
$L_O$	Number of time frames in the future trajectory
$\ell(\cdot)$	Loss function
$\lambda$	Regularization coefficient
$\hat{h}$	A given deployed ML model
$\epsilon_t$	Observed prediction error at time $t$
$g_\theta(\epsilon_t)$	Post-change distribution parameterized by $\theta$
$f_\phi(\epsilon_t)$	Pre-change distribution parameterized by $\phi$
$\gamma$	Change-point at which the distribution shifts from $f_\phi$ to $g_\theta$ .
$\tau$	Stopping time at which a change is detected
$b$	Detection threshold that controls sensitivity to change detection
$W_t$	CUSUM statistic at time $t$
$\eta$	True gap between the post-change and pre-change distributions
$\kappa$	Assumed shift value used to evaluate robustness
$\mathcal{P}_1$	The set of all possible $\hat{g}_\theta$ obtained by shifting the $f_\phi(\epsilon_t)$ , $\mathcal{P}_1 = \{f_\phi(\epsilon_t - \eta) \mid \eta \geq \kappa\}$
$\mathcal{P}_2$	The convex hull of $\mathcal{P}_1$ , $\mathcal{P}_2 = \text{conv}(\mathcal{P}_1)$

### 3 PROBLEM FORMULATION

#### 3.1 Trajectory Representation and the Prediction Problem

The training dataset  $\mathcal{D} = \{S_j\}_{j=1}^N$  is a collection of driving scenes. Each  $S_j$  described by a triple  $S_j = (\mathcal{X}_j, \mathcal{Y}_j, \mathcal{M})$ , where  $\mathcal{X}_j$  is the collections of observed trajectories,  $\mathcal{Y}_j$  is the collection of future trajectories that we aim to predict based on  $\mathcal{X}_j$ , and  $\mathcal{M}$  is the map information. When a dataset does not have map information, we set  $\mathcal{M} = \emptyset$ . In a driving scene, an agent represents a moving object such as a vehicle, a motorcycle, or a pedestrian. For a given driving scene  $S_j$ , let  $m_j$  denote the number of agents in the scene. Hence,  $\mathcal{X}_j$  and  $\mathcal{Y}_j$  can be explicitly written out as  $\mathcal{X}_j = \{x_j^1, \dots, x_j^{m_j}\}$  and  $\mathcal{Y}_j = \{y_j^1, \dots, y_j^{m_j}\}$ , where  $x_j^i \in \mathbb{R}^{2 \times L_I}$  and  $y_j^i \in \mathbb{R}^{2 \times L_O}$  for each agent  $i$  in the scene. Here,  $L_I$  and  $L_O$  are the numbers of time frames in the observed trajectory  $x_j^i$  and in the future trajectory  $y_j^i$ , respectively. It is worth noting that:

- (1) Different from traditional supervised learning problem, in the trajectory prediction problem, the trajectory of an agent is a sequence of positions, resulting in possibly often overlapping  $\mathcal{X}_j$  and  $\mathcal{Y}_j$ .
- (2) Different driving scenes may contain different numbers of agents as can be seen in Fig. 1.

A machine-learning model  $\hat{h}$  for the trajectory prediction task can be trained by minimizing the objective function that may take the form

$$\min_f \frac{1}{N} \sum_{j=1}^N \ell(\hat{h}(X_j), Y_j) + \lambda \times \text{regularization},$$

where  $\ell$  is a loss function such as the negative log-likelihood (NLL) of the Laplace/Gaussian distributions [50, 64],  $\lambda \geq 0$  is the regularization coefficient, and one popular choice of the regularization term in the objective is the cross entropy loss.

The specific training methods are out of the scope of this paper. Readers can find concrete instances of the objective functions in [50, 64] and others. Notably, different from traditional machine learning tasks, where the model trained has fixed input and output dimensions, the trajectory prediction model [64]  $\hat{h}$  may have varying input and output dimensions.

**Evaluation Metrics.** Let  $\hat{h}$  be a given deployed trajectory prediction model. We follow existing literature on trajectory prediction model training to evaluate the generalization performance of  $\hat{h}$  [9, 73]. Let  $\mathcal{D}_{\text{test}} = \{\mathcal{S}_j\}_{j=1}^{N_{\text{test}}}$  be the test dataset. Instead of evaluating the trajectory prediction errors of all neighboring agents, only the prediction errors on an arbitrarily chosen agent will be evaluated. Such chosen agent is referred to as *target agent* of scene  $\mathcal{S}_j$ , denoted as  $t_j$ . We use three common metrics in trajectory prediction: *Average displacement error* (ADE) and *Final displacement error* (FDE) and *Root Mean Squared Error* (RMSE). These metrics are widely adopted in prior works [11, 27], including the ICRA 2020 *nuScenes* prediction challenge [23, 38].

- **ADE** measures the average error over the entire prediction horizon:

$$\text{ADE} := \frac{1}{N_{\text{test}}} \sum_{j=1}^{N_{\text{test}}} \frac{1}{L_O} \|\hat{h}(x_j^{t_j}) - y_j^{t_j}\|_2,$$

- **FDE** captures the error at the final time step of the predicted trajectory:

$$\text{FDE} := \frac{1}{N_{\text{test}}} \sum_{j=1}^{N_{\text{test}}} \frac{1}{L_O} \|\hat{h}(x_j^{t_j})_{L_O} - [y_j^{t_j}]_{L_O}\|_2,$$

where  $[\hat{h}(x_j^{t_j})]_{L_P}$  and  $[y_j^{t_j}]_{L_P}$  are the last positions in  $\hat{h}(x_j^{t_j})$  and  $y_j^{t_j}$ , respectively.

- **RMSE** computes the square root of the average squared differences between predicted and true positions over the prediction window:

$$\text{RMSE}_t := \frac{1}{N_{\text{test}}} \sum_{j=1}^{N_{\text{test}}} \sqrt{\frac{1}{L_O} \|\hat{h}(x_j^{t_j}) - y_j^{t_j}\|_2^2}.$$

### 3.2 Casting OOD Awareness as a QCD Problem

In the context of trajectory prediction, we define OOD awareness as the ability to detect deviations in prediction performance over time. Specifically, we consider a sequence of prediction errors  $\epsilon_t$  arising from a trajectory prediction model  $\hat{h}$ . The sequence of errors is defined as

$$\epsilon_t = d(\hat{h}(X_t), Y_t), \quad (1)$$

where  $d(\cdot, \cdot)$  is a distance function measuring the discrepancy between the predicted future trajectory and the ground truth. As mentioned in Section 3.1, we consider three distance functions, *i.e.*, ADE, FDE, and RMSE.

The AV observes the sequence  $\{\epsilon_t\} = \{\epsilon_1, \epsilon_2, \dots, \epsilon_t\}$  of the target agent ( $a$ ) for every scene. Let the data distribution change at an unknown time  $\gamma$ . We denote the pre-change distribution of  $\epsilon_t$  by  $f_\phi(\epsilon_t)$  for  $t < \gamma$  and the post-change distribution by  $g_\theta(\epsilon_t)$  for  $t \geq \gamma$ , i.e.,

$$\epsilon_t \sim \begin{cases} f_\phi(\epsilon_t), & t < \gamma \text{ (ID Scene)}, \\ g_\theta(\epsilon_t), & t \geq \gamma \text{ (OOD Scene)}. \end{cases} \quad (2)$$

Let  $\mathcal{A}$  be any algorithm. Let  $\tau_{\mathcal{A}}$  be the time that a change is declared under algorithm  $\mathcal{A}$ . When the adopted  $\mathcal{A}$  is clear from the context, we drop the subscript  $\mathcal{A}$  in  $\tau$ . Two key metrics for evaluating OOD detection algorithms are: (1) *Detection Delay*—time to detect an OOD event, reflecting responsiveness; and (2) *False Alarm Rate*—frequency of incorrect OOD flags, ensuring reliability. These metrics are widely used in [28, 29, 36] due to their ability to capture the trade-off between sensitivity and robustness.

For any  $\gamma < \infty$ , a true detection happens if  $\tau \geq \gamma$  and false if  $\tau < \gamma$ . The design of the quickest change detection procedures involves optimizing the tradeoff between the delay to detection  $(\tau - \gamma + 1)^+$  and false alarm.

To ensure robust safety guarantees, we follow Lorden’s minimax formulation [40], which quantifies the detection delay using the Worst-Case Average Detection Delay (WADD),

$$\text{WADD}(\tau) = \sup_{t \geq 1} \text{ess sup } \mathbb{E}_t[(\tau - \gamma + 1)^+ \mid \epsilon_1, \dots, \epsilon_{t-1}], \quad (3)$$

where  $(\cdot)^+ = \max\{0, \cdot\}$ ,  $\mathbb{E}_t[\cdot]$  denotes the expectation when the change occurs at time  $t$ , and  $\text{ess sup}(\cdot)$  refers to the essential supremum of a scalar random variable.

The metric of false alarm can be measured by the false alarm rate  $\text{FAR}(\tau)$  [71] or by the mean time to false alarm  $\text{MTFA}(\tau)$ , i.e.,

$$\text{FAR}(\tau) = \frac{1}{\mathbb{E}_\infty(\tau)} \quad \text{and} \quad \text{MTFA}(\tau) = \mathbb{E}_\infty[\tau \mid \tau < \gamma]. \quad (4)$$

where  $\mathbb{E}_\infty$  denotes the expectation when the change never occurs.

## 4 PRELIMINARIES

This section provides the preliminaries for our OOD awareness algorithms. In Section 4.1, we outline the high-level approach for generating deceptive OOD scenes in our experiments. In Section 4.2, we present preliminary experimental observations on the statistical structure of the pre- and post-change distributions.

### 4.1 Deceptive OOD Scene Generation

Deceptive OOD scenes refer to driving scenarios where deviations from expected behavior are subtle and difficult to identify, even for human observers. Unlike easily detectable OOD events such as sudden acceleration or erratic lane changes, deceptive OOD scenes maintain motion patterns that fall within normal variations, making them particularly challenging to recognize. These scenarios can arise from minor trajectory shifts of neighboring vehicles due to environmental factors such as road debris, unexpected pedestrian movements, or subtle driver behaviors.

To systematically generate deceptive OOD scenes, we adopt the adversarial perturbation framework proposed by [76]. Fig. 3 illustrates the process of introducing controlled modifications to historical trajectory data while ensuring the altered trajectories remain physically plausible. In particular, we use the single-frame perturbation method in [76], i.e., perturbing only  $L_p = 1$  time-frame among the  $L_l$  history trajectory time-frames. Fig. 4 provides a comparative visualization of AV trajectory prediction performance in normal (ID) and perturbed (OOD) scene, highlighting why deceptive OOD cases pose a greater hazard than one might expect. In the ID setting (left), the ego vehicle (gray car)

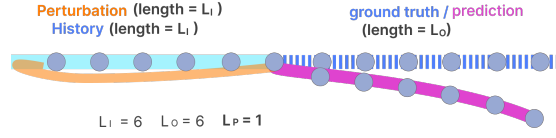


Fig. 3. Visualization of minor perturbation applied to the history trajectory of the target vehicle. The input and output trajectories consist of  $L_I = 6$  and  $L_O = 6$  time frames, respectively, while  $L_P = 1$  denotes the perturbed time frame within the input. Dots represent observed and predicted trajectory positions at different time frames.

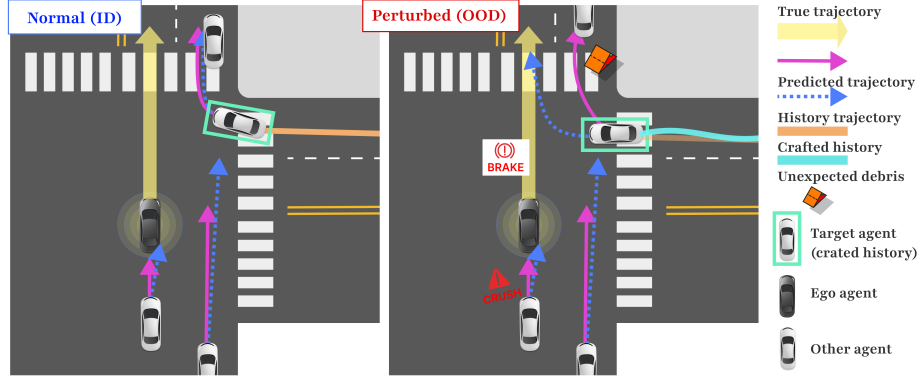


Fig. 4. Illustration of the performance comparison of a given ML trajectory prediction model on ID and OOD scenes. In an ID scenario (left figure), the ego vehicle (gray car), on which the ML model is implemented, can accurately predict the trajectories of neighboring vehicles. In an OOD scenario (right figure), the target vehicle slightly deviates from its usual driving path due to unexpected debris from the vehicle ahead. As a result, the ego vehicle may mispredict the target vehicle's trajectory, mistakenly assuming it will move into the same lane. In response, the ego vehicle may suddenly brake, potentially causing a rear-end collision.

accurately predicts the trajectories of surrounding vehicles, maintaining safe driving behavior. However, in the OOD setting (right), the target vehicle undergoes a subtle deviation due to an external factor, such as an obstacle ahead. Although the deviation is minor, it causes the ego vehicle's ML model to mispredict the target's future path, leading to an unnecessary sudden brake maneuver. This reaction could result in a rear-end collision.

#### 4.2 Gaussian Mixture of Pre- and Post-Change Distributions

Understanding the statistical structure of trajectory prediction errors is critical for detecting meaningful changes in autonomous driving systems. To address this, we analyze the pre- and post-change distributions of these errors using real-world datasets. Our key observation is that the data is approximately represented by a *Gaussian mixture model* (GMM). As illustrated in Fig. 5, the GMM fits for pre- and post-change ADE distributions in the ApolloScape dataset. Fig. 5a presents results from the GRIP++ model, while Fig. 5b depicts outcomes from the FQA model. Similar trends were consistently observed across other datasets (e.g., NGSIM and nuScenes) and for additional metrics (e.g., FDE and RMSE), though these results are omitted due to space constraints.

### 5 METHODS

In this section, we present the key methods used for detecting OOD scenes, focusing on CUSUM as the primary algorithm, with Z-Score and Chi-Square tests serving as benchmark comparisons. CUSUM is a mature method known

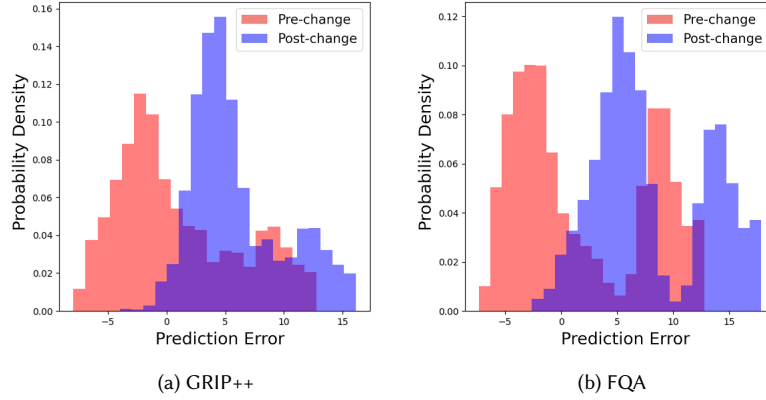


Fig. 5. Illustration of the mixture Gaussian distributions for pre-change (red) and post-change (blue) error distributions in trajectory prediction, assessed using the ADE metric on the ApolloScape dataset. (a) Results from the GRIP++ model. (b) Results from the FQA model. Both examples highlight the observed shift in error distributions.

for its robust theoretical foundation and ability to quickly and reliably detect distributional shifts [43, 61]. In particular, CUSUM is designed to minimize detection delay while keeping the false alarm rate within acceptable bounds, providing formal performance guarantees in dynamic environments. As benchmarks, the Z-Score and Chi-Square methods are commonly used in literature for comparison [4, 5, 44, 72].

### 5.1 Background of CUSUM

As discussed in Section 3.2, we denote the unknown change point by  $\gamma$ , while  $t_0$  represents the current system time, incrementing by 1 at each time step. The problem of detecting OOD can be formulated as detecting a shift in the distribution of the prediction errors  $\{\epsilon_t\}$ . As shown in Fig. 3, we observe that on some popular datasets of trajectory prediction, the pre- and post-change distributions are Gaussian mixtures with two components. We evaluate the CUSUM algorithm under three common scenarios (Section 5.2.1, Section 5.2.2, and Section 5.2.3).

The CUSUM algorithm detects distributional shifts by monitoring cumulative deviations in the log-likelihood ratio between pre-change ( $f_\phi$ ) and post-change ( $g_\theta$ ) distributions. The decision statistic  $W_t$  is computed iteratively

$$W_t = \begin{cases} 0, & \text{if } t = 0, \\ \max(W_{t-1} + \log L(\epsilon_t), 0), & \text{if } t \geq 1, \end{cases} \quad (5)$$

where  $L(\epsilon_t) = \frac{g_\theta(\epsilon_t)}{f_\phi(\epsilon_t)}$  is the likelihood ratio. A change is declared when  $W_t$  exceeds a threshold  $b$

$$\tau = \inf\{t \geq 1 : W_t \geq b\}.$$

This method optimally balances the trade-off between false alarm rate  $\text{FAR}(\tau < \gamma)$  and detection delay  $\mathbb{E}[\tau - \gamma \mid \tau \geq \gamma]$ . This method enables awareness of sequential decision reliability by continuously monitoring prediction errors. For implementation details, see Algorithm 1.

**Algorithm 1:** Ideal CUSUM with Parameterized Models**Input:** Threshold  $b > 0$ ; pre-change distribution  $f_\phi(\epsilon_t)$ ; post-change distribution  $g_\theta(\epsilon_t)$ **Output:** Change point  $\tau$  if detectedInitialize  $W_0 \leftarrow 0$ ;**while** *true* **do**    get a new observation of the prediction error  $\epsilon_t$ ;

/\* Compute the log-likelihood ratio

\*/

$$L(\epsilon_t) = \frac{g_\theta(\epsilon_t)}{f_\phi(\epsilon_t)}$$

 $W_{t+1} \leftarrow \max(W_t + \log L(\epsilon_t), 0)$ ;    **if**  $W_{t+1} \geq b$  **then**

Declare a change point;

**return**  $\tau = t + 1$ ;

**THEOREM 1** ([71]). *The CUSUM test is optimal for minimizing WADD given in (4) subject to any fixed constraint of  $\alpha$  on FAR given in (4). In addition, for any  $\alpha \in (0, 1)$ , setting the threshold  $b = |\log \alpha|$  ensures*

$$\text{FAR}(\tau) \leq \alpha \quad \text{and} \quad \text{WADD}(\tau) = \frac{|\log \alpha|}{D_{KL}(g_\theta, f_\phi)} (1 + o(1)),$$

as  $\alpha \rightarrow 0$ , where  $D_{KL}(g_\theta, f_\phi)$  is the Kullback-Leibler divergence between pre-change and post-change distributions.

**Rationale.** After a change-point  $\gamma$ , the observations  $\epsilon_t$  are distributed according to  $g_\theta$ , and the expected log-likelihood ratio  $\mathbb{E}_{t \geq \gamma}[\log(\frac{g_\theta(\epsilon_t)}{f_\phi(\epsilon_t)})]$  equals the Kullback-Leibler divergence  $D_{KL}(g_\theta \parallel f_\phi)$ , which is positive. Conversely, before  $\gamma$ , the observations are governed by  $f$ , and  $\mathbb{E}_{t < \gamma}[\log(\frac{g_\theta(\epsilon_t)}{f_\phi(\epsilon_t)})] = -D_{KL}(f_\phi \parallel g_\theta)$ , which is negative. Consequently, with an increasing number of observations, the cumulative sum  $\sum_{t: t \geq \gamma} \log(\frac{g_\theta(\epsilon_t)}{f_\phi(\epsilon_t)})$  is expected to exceed the threshold  $b$ . The  $\max\{\cdot, 0\}$  function in the statistic  $W_t$  keeps the statistic from going to  $-\infty$  when the change time is large. The threshold  $b$  controls the sensitivity of the detection; increasing  $b$  makes the algorithm less prone to false alarms but also delays the detection of actual changes.

## 5.2 CUSUM for OOD Scene Detection

In this subsection, we present several variants of the CUSUM tests, each differing in its requirements for prior knowledge of the pre- and post-change distributions. Section 5.2.1 presents the ideal CUSUM test where both pre- and post-change distributions are fully known and provided as inputs to the algorithm. Section 5.2.2 describes two tests that require only partial knowledge of the pre- and/or post-change distributions. Section 5.2.3 introduces a test that does not require any knowledge on the post-change distribution.

**5.2.1 CUSUM with Complete Knowledge.** From Section 4.2, we know that both the pre-change ( $f_\phi$ ) and post-change ( $g_\theta$ ) distributions follow GMMs. The probability density function for GMM can be defined as  $p(\epsilon_t) = \sum_{i=1}^K w_i \cdot \mathcal{N}(\epsilon_t \mid \mu_i, \sigma_i^2)$ , where  $K$  is the number of Gaussian components in the mixture, and  $w_i$ ,  $\mu_i$ , and  $\sigma_i^2$ , respectively, are the mixture weight, the mean, and the variance of component  $i$ .

In our experimental results in Fig. 3, we run Algorithm 1 by plugging in the Gaussian mixture pdfs obtained from Section 4.2 where  $K = 2$ . Since this method is only a concrete instance of the ideal CUSUM, Theorem 1 is applicable, *i.e.*, this method is optimal.



**5.2.2 CUSUM with Partial Knowledge.** In many real-world applications, post-change distributions are difficult to characterize precisely. Occasionally, in some cases, even pre-change distributions may be challenging to obtain. In those cases, we need to approximate the post- or/and pre-change distributions. However, not all approximations are correct. We use the following definition to formalize the notion of correctness for OOD detection.

*Definition 2.* [Approximation correctness] Let  $\hat{L}(\epsilon_t)$  be the likelihood approximation used. Let  $\hat{W}$  denote the CUSUM statistic defined as  $\hat{W}_{t+1} = \max(\hat{W}_t + \log \hat{L}(\epsilon_t), 0)$  with  $\hat{W}_0 = 0$ . We say the approximation  $\hat{L}$  is correct if for any finite-time change-point  $\gamma < \infty$ ,

$$\mathbb{E}_{t < \gamma} [\log \hat{L}(\epsilon_t)] < 0, \text{ and } \mathbb{E}_{t \geq \gamma} [\log \hat{L}(\epsilon_t)] > 0.$$

Intuitively,  $\mathbb{E}_{t < \gamma} [\log \hat{L}(\epsilon_t)] < 0$  prevents an overwhelming number of false alarms before a change occurs, while  $\mathbb{E}_{t \geq \gamma} [\log \hat{L}(\epsilon_t)] > 0$  ensures that once a change occurs, it will be detected eventually.

Partial knowledge of post-change. The exact parameters of the post-change distribution are often unknown. Instead, we leverage partial knowledge or side information to approximate the post-change distributions. In particular, we consider the case when the overall mean  $\mu_g$  and variance  $\sigma_g^2$  of the post-change distribution are known. We use  $\mathcal{N}(\epsilon_t | \mu_g, \sigma_g^2)$  – a single Gaussian distribution with the given mean and variance – to replace the true post-change distribution  $g_\theta$  in computing the likelihood ratio in (5), i.e.,

$$L(\epsilon_t) = \frac{\hat{g}_\theta(\epsilon_t)}{f_\phi(\epsilon_t)}, \text{ where } \hat{g}_\theta(\epsilon_t) = \mathcal{N}(\epsilon_t | \mu_g, \sigma_g^2).$$

Let  $W_t^{p1}$  denote the CUSUM statistic with the above approximation, i.e.,

$$W_t^{p1} = \max \left( 0, W_{t-1}^{p1} + \log \frac{\hat{g}_\theta(\epsilon_t)}{f_\phi(\epsilon_t)} \right), \quad W_0^{p1} = 0. \quad (6)$$

**Rationale.** To ensure correctness as per Definition 2, one needs to check

$$\mathbb{E}_{t \geq \gamma} [\log(\frac{\hat{g}_\theta(\epsilon_t)}{f_\phi(\epsilon_t)})] > 0, \text{ and } \mathbb{E}_{t < \gamma} [\log(\frac{\hat{g}_\theta(\epsilon_t)}{f_\phi(\epsilon_t)})] < 0.$$

Note that  $\mathbb{E}_{t < \gamma} [\log(\frac{\hat{g}_\theta(\epsilon_t)}{f_\phi(\epsilon_t)})] = \int_{\epsilon} f_\phi(\epsilon) \frac{\hat{g}_\theta(\epsilon)}{f_\phi(\epsilon)} d\epsilon = -D_{KL}(f_\phi \| \hat{g}_\theta) < 0$ . In addition, it holds that

$$\begin{aligned} \mathbb{E}_{t \geq \gamma} [\log(\frac{\hat{g}_\theta(\epsilon_t)}{f_\phi(\epsilon_t)})] &= \int_{\epsilon} g_\theta(\epsilon) \log \frac{\hat{g}_\theta(\epsilon)}{f_\phi(\epsilon)} d\epsilon = \int_{\epsilon} g_\theta(\epsilon) \log \frac{g_\theta(\epsilon)}{f_\phi(\epsilon)} \frac{\hat{g}_\theta(\epsilon)}{g_\theta(\epsilon)} d\epsilon \\ &= D_{KL}(g_\theta(\epsilon) \| f_\phi(\epsilon)) - D_{KL}(g_\theta(\epsilon) \| \hat{g}_\theta(\epsilon)). \end{aligned}$$

In general, the sign of  $\mathbb{E}_{t \geq \gamma} [\log(\frac{\hat{g}_\theta(\epsilon_t)}{f_\phi(\epsilon_t)})]$  is undetermined, and depends on the relative magnitudes of  $D_{KL}(g_\theta(\epsilon) \| f_\phi(\epsilon))$  and  $D_{KL}(g_\theta(\epsilon) \| \hat{g}_\theta(\epsilon))$ . Fortunately, as shown in Table 2, in our experiments, its sign is consistently positive across metrics and models, with full numerical analysis presented in Section 6.2.

Table 2. Numerical evaluation of  $\mathbb{E}_{t \geq \gamma} [\log(\frac{\hat{g}_\theta(\epsilon_t)}{f_\phi(\epsilon_t)})]$  under the FQA model, using ApolloScape dataset and ADE metric.

	$\mathbb{E}_{t \geq \gamma} [\log(\frac{\hat{g}_\theta(\epsilon_t)}{f_\phi(\epsilon_t)})]$		
Components	$D_{KL}(g_\theta \  f_\phi)$	$D_{KL}(g_\theta \  \hat{g}_\theta)$	sign of difference
Values	0.2026	0.0405	positive

Partial knowledge of both pre- and post-change. Occasionally, the pre-change distribution may not be known, which may result from a lack of sufficient data to reconstruct the true distribution. We consider the case when the overall means ( $\mu_f$  and  $\mu_g$ ) and variances ( $\sigma_f^2$  and  $\sigma_g^2$ ) of pre- and post-change distributions are known. We use single Gaussians to approximate the pre- and post-change distributions in computing the likelihood ratio in (5), i.e.,

$$L(\epsilon_t) = \frac{\hat{g}_\theta(\epsilon_t)}{\hat{f}_\phi(\epsilon_t)},$$

where  $\hat{f}_\theta(\epsilon_t) = \mathcal{N}(\epsilon_t | \mu_f, \sigma_f^2)$  and  $\hat{g}_\theta(\epsilon_t) = \mathcal{N}(\epsilon_t | \mu_g, \sigma_g^2)$ . Let  $W_t^{p2}$  denote the CUSUM statistic, i.e.,

$$W_t^{p2} = \max \left( 0, W_{t-1}^{p2} + \log \frac{\hat{g}_\theta(\epsilon_t)}{\hat{f}_\phi(\epsilon_t)} \right), \quad W_0^{p2} = 0. \quad (7)$$

**Rationale.** Different from the case when pre-change distribution is known, here the signs of  $\mathbb{E}_{t \geq \gamma} [\log(\frac{\hat{g}_\theta(\epsilon_t)}{\hat{f}_\phi(\epsilon_t)})]$  and  $\mathbb{E}_{t < \gamma} [\log(\frac{\hat{g}_\theta(\epsilon_t)}{\hat{f}_\phi(\epsilon_t)})]$  are not generally predetermined. In particular,

$$\mathbb{E}_{t \geq \gamma} [\log(\frac{\hat{g}_\theta(\epsilon_t)}{\hat{f}_\phi(\epsilon_t)})] = D_{KL}(g_\theta \| \hat{f}_\phi) - D_{KL}(g_\theta \| \hat{g}_\theta), \text{ and } \mathbb{E}_{t < \gamma} [\log(\frac{\hat{g}_\theta(\epsilon_t)}{\hat{f}_\phi(\epsilon_t)})] = -D_{KL}(f_\phi \| \hat{g}_\theta) + D_{KL}(f_\phi \| \hat{f}_\phi).$$

Fortunately, in our experiments, the former is  $>0$  and the latter  $<0$ , satisfying the correctness criterion in Definition 2.

Table 3. Numerical evaluation of  $\mathbb{E}_{t < \gamma} [\log(\frac{\hat{g}_\theta(\epsilon_t)}{\hat{f}_\phi(\epsilon_t)})]$  and  $\mathbb{E}_{t \geq \gamma} [\log(\frac{\hat{g}_\theta(\epsilon_t)}{\hat{f}_\phi(\epsilon_t)})]$  under the FQA model, using ApolloScope dataset and ADE metric.

	$\mathbb{E}_{t < \gamma} [\log(\frac{\hat{g}_\theta(\epsilon_t)}{\hat{f}_\phi(\epsilon_t)})]$			$\mathbb{E}_{t \geq \gamma} [\log(\frac{\hat{g}_\theta(\epsilon_t)}{\hat{f}_\phi(\epsilon_t)})]$		
Cases	$D_{KL}(f_\phi \  \hat{f}_\phi)$	$D_{KL}(f_\phi \  \hat{g}_\theta)$	sign of difference	$D_{KL}(g_\theta \  \hat{f}_\phi)$	$D_{KL}(g_\theta \  \hat{g}_\theta)$	sign of difference
Values	0.3584	0.4044	negative	0.2885	0.0405	positive

**5.2.3 CUSUM with Unknown Knowledge on Post-change Distribution.** Now, we consider the setting where no information about the post-change distribution is available for constructing an approximation of the likelihood ratio  $L(\epsilon_t) = \frac{g_\theta(\epsilon_t)}{f_\phi(\epsilon_t)}$ . We propose a robust CUSUM test that accommodates such a lack of knowledge based on the notion of the least favorable distribution. Analysis of the actual pre- and post-change data (see Fig. 5) of trajectory prediction suggests that often the post-change GMM is an approximately location-shifted version of the pre-change GMM. Motivated by this, we design our robust test based on the notion of minimum shift. Specifically, we use the available data to learn the pre-change model  $f_\phi(\epsilon_t)$ . We then design the robust CUSUM test by selecting  $f_\phi(\epsilon_t - \kappa)$  as the approximation of the post-change distribution, where  $\kappa$  is a putative choice for the distributional shift. This gives us the CUSUM statistic

$$W_t^{(\kappa)} = \max \left( 0, W_{t-1}^{(\kappa)} + \log \frac{f_\phi(\epsilon_t - \kappa)}{f_\phi(\epsilon_t)} \right), \quad W_0^{(\kappa)} = 0. \quad (8)$$

The shift parameter  $\kappa$  can be chosen either using prior knowledge or based on the standard deviation of the pre-change model. Below, we prove that this test is robustly optimal under certain assumptions on the actual post-change distribution.

Define the following classes of post-change distributions:

$$\begin{aligned} \mathcal{P}_1 &= \{f_\phi(\epsilon_t - \eta) : \eta \geq \kappa\} \\ \mathcal{P}_2 &= \text{convex hull}(\mathcal{P}_1). \end{aligned} \quad (9)$$

Thus,  $\mathcal{P}_1$  collects all possible post-change distributions that are a shifted version of the pre-change model, with the shift  $\eta$  being more than the shift  $\kappa$  used to design the test in (8). The family  $\mathcal{P}_2$  is the convex hull (finite convex combinations) of the distributions in  $\mathcal{P}_1$ . Next, consider the following robust optimization formulation:

$$\begin{aligned} \min_{\tau} \quad & \sup_{P \in \mathcal{P}} \text{WADD}^P(\tau) \\ \text{subject to} \quad & \text{FAR}(\tau) \leq \alpha, \end{aligned} \quad (10)$$

where  $\text{WADD}^P(\tau)$  is the delay when the post-change distribution is  $P$ . The family  $\mathcal{P}$  can be either  $\mathcal{P} = \mathcal{P}_1$  or  $\mathcal{P} = \mathcal{P}_2$  defined in (9). We now state our main result on robust optimality.

**THEOREM 3.** *The CUSUM algorithm in (8) is asymptotically robust optimal for the problem in (10) for  $\mathcal{P} = \mathcal{P}_1$  or  $\mathcal{P} = \mathcal{P}_2$  as  $\alpha \rightarrow 0$ .*

**PROOF.** The minimal shift distribution  $f_\phi(\epsilon_t - \eta)$  satisfies the weak stochastic boundedness conditions (14) and (15) given in [46]. The theorem then follows from Theorem 3 in [46].  $\square$

We remark that the robust test is approximately correct, according to Definition 2, for every possible post-change law in  $\mathcal{P}_1$  and  $\mathcal{P}_2$ .

It is important to choose the minimal shift  $\kappa$  carefully in (8). In Fig. 6, we compare the performance of the robust CUSUM test with other nonrobust CUSUM tests. A non-robust CUSUM test is one where the shift chosen is too large and hence affected underperforms. In the figures,  $\kappa = 1$ , and the actual post-change corresponds to a shift of 2.5.

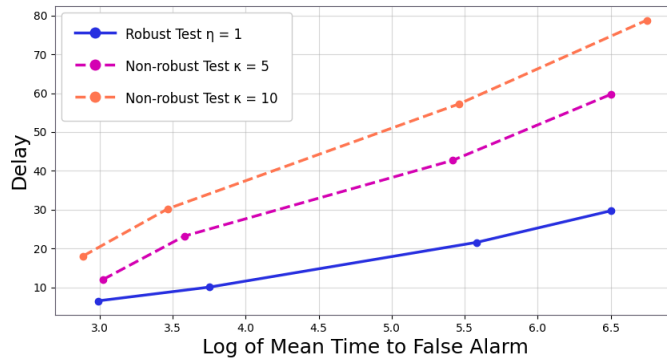


Fig. 6. For the actual gap  $\eta = 2.5$ , we set the minimum test shift parameter to  $\kappa = 1$  to evaluate robustness. The robust test (blue curve) with shift = 1 achieves successful detection, validating its effectiveness. In contrast, the non-robust tests (pink curve with shift = 5 and orange curve with shift = 10) fail to maintain detection capability, as their parameter choices violate the robustness criteria.

### 5.3 Benchmarks

**5.3.1 Z-Score Time-series Detection.** The Z-Score method detects change points by measuring how much a data point deviates from a moving average. For any given window size  $w$ , define the moving average as  $\bar{\epsilon}_t := \frac{1}{w} \sum_{r=t-w+1}^t \epsilon_r$ , and the moving standard deviation as  $\sigma_t = \sqrt{\frac{1}{w} \sum_{r=t-w+1}^t (\epsilon_r - \bar{\epsilon}_t)^2}$ . The Z-score of  $\epsilon_t$  is

$$z_t = \frac{\epsilon_t - \bar{\epsilon}_t}{\sigma_t} \quad (11)$$

A threshold  $b$  is set for the Z-Score, often based on how sensitive the detection should be. When the absolute value of the Z-Score  $|z_t|$  exceeds the threshold, the Z-Score method declares that a change has occurred. That is,

$$\tau = \min\{t : |z_t| > b\}.$$

**5.3.2 Chi-Square Time-series Detection.** Chi-Square test is commonly used to evaluate the independence of categorical variables and the fit between observed and expected frequencies. Specifically, we use Pearson’s chi-square test to compare observed frequencies in the time-series with expected frequencies under normal behavior [15]. Significant deviations from the expected values suggest potential anomalies. The test statistic is computed as follows:  $\chi_t^2 = \sum_{r=t-w+1}^t \frac{(g_\theta(\epsilon_t) - f_\phi(\epsilon_t))^2}{f_\phi(\epsilon_t)}$ , where  $w$  represents the window size. The null hypothesis assumes no significant difference between the frequencies. A large  $\chi^2$  value indicates an anomaly, and a change is declared when  $\chi^2$  exceeds a predefined threshold. For any given  $b$ , a change is declared accordingly to the following rule

$$\tau = \min\{t : \chi_t^2 > b\}.$$

## 6 EXPERIMENTS AND RESULTS

### 6.1 Simulation Setup

**Datasets.** Table 4 summarizes the characteristics of the three datasets used. The ApolloScape [20], NGSIM [13], and NuScenes [3] datasets are widely used in trajectory prediction and autonomous vehicle research due to their diverse and complex real-world driving scenes. ApolloScape provides a rich multimodal dataset, including camera images, LiDAR point clouds, and approximately 50 minutes of manually annotated vehicle trajectories. NGSIM focuses on freeway traffic behavior, offering detailed vehicle trajectories recorded over 45 minutes on highways US-101 and I-80. NuScenes captures 1000 diverse driving scenes in Boston and Singapore, two cities known for their challenging traffic conditions. For trajectory prediction, we choose the history trajectory length ( $L_I$ ) and future trajectory length ( $L_O$ ) based on the recommendations provided by the dataset’s authors. For each dataset, we randomly select 2500 scenes to serve as test cases.

Table 4. Summary of datasets.

Name	Scenario	Map	$L_I$	$L_O$
ApolloScape [20]	Urban	×	6	6
NGSIM [13]	Highway	×	15	25
NuScenes [3]	Urban	✓	4	12

Table 5. Summary of models.

Name	Input features	Output format	Network
GRIP++ [34]	location + heading	single-prediction	Conv + GRU
FQA [26]	location	single-prediction	LSTM

**Trajectory Prediction Models.** Table 5 summarizes two benchmark models used for trajectory prediction. We select GRIP++ [34] and FQA[26] as our trajectory prediction models due to their proven effectiveness on widely used datasets like ApolloScape and NGSIM from prior research. GRIP++ employs a graph-based structure with a two-layer GRU network, offering fast and accurate short- and long-term predictions, ranking #1 in the 2019 ApolloScape competition, making it an ideal fit for our experiments by minimizing model noise and enhancing algorithm performance evaluation.

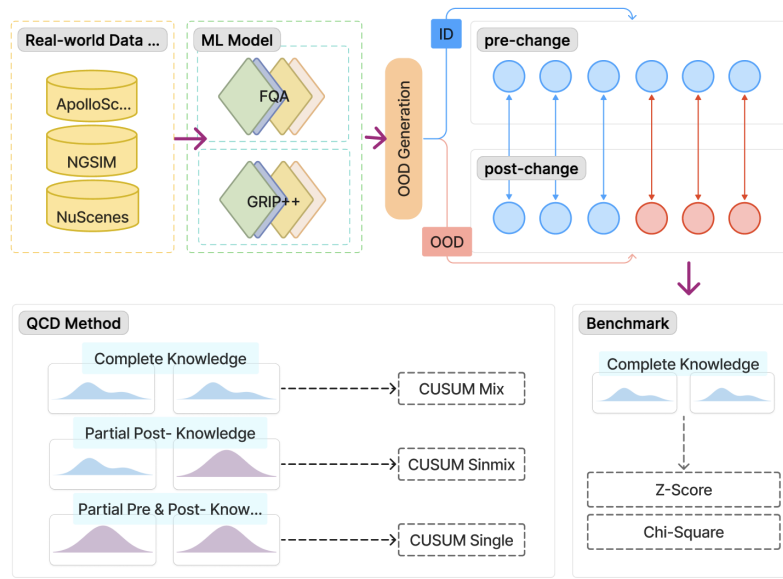


Fig. 7. Workflow of OOD detection in trajectory prediction. The process includes data loading, model training, OOD generation, and OOD detection using CUSUM variants and statistical benchmarks.

FQA introduces a fuzzy attention mechanism to model dynamic agent interactions, showing strong performance across diverse domains, including traffic and human motion which is well-suited for evaluating prediction performance in nuScenes dataset.

**Deceptive OOD Scene Generation.** We generate deceptive OOD scenes by introducing subtle, physically constrained changes in driving behaviors. These changes, often imperceptible to human observers, are designed to significantly degrade the prediction performance of machine learning models. Inspired by adversarial perturbation techniques [76], we apply these perturbations in a single-frame prediction setting for each dataset-model combination. The results, presented in Table 6, demonstrate that such perturbations consistently worsen trajectory prediction accuracy. On average, ADE increases by 148.8%, FDE by 176.2%, and RMSE by 50.1%. Notably, FDE experiences the highest increase (176.2%), highlighting greater vulnerability in long-term predictions compared to short-term or overall error measures. These findings suggest that even minor trajectory shifts could have real-world consequences if OOD scenes cannot be detected.

Table 6. Average prediction error before and after the perturbation.

Model	Dataset	ADE (m)	FDE (m)	RMSE (m)
GRIP++	ApolloScape	1.68 / 4.15	2.11 / 8.73	6.16 / 6.26
	NGSIM	4.35 / 7.89	7.50 / 14.82	1.23 / 3.36
	NuScenes	5.82 / 8.16	5.03 / 8.78	5.74 / 5.33
FQA	ApolloScape	1.87 / 4.95	2.91 / 9.53	6.96 / 6.53
	NGSIM	4.63 / 8.69	7.88 / 15.62	1.63 / 4.16
	NuScenes	6.62 / 8.96	5.83 / 9.58	6.54 / 6.13

**Workflow Design.** Fig. 7 illustrates our experimental workflow, which consists of four main stages: data loading, model training, OOD generation, and OOD detection. For each model-dataset combination (summarized in Tables 4 and 5), trajectory predictions for both ID and OOD scenarios are generated following [76]. The resulting prediction error sequences are fitted into pre-change ( $f_\phi$ ) and post-change ( $g_\theta$ ) distributions. As discussed in Section 5.2, the performance of the CUSUM algorithm varies based on the level of prior knowledge about  $f_\phi$  and  $g_\theta$ . To address different scenarios, we employ following CUSUM variants for OOD detection and compared with benchmarks (*i.e.*, Z-Score [4] and Chi-Square [54]):

- **CUSUM Mix:** Assumes full knowledge of both  $f_\phi$  and  $g_\theta$ , modeling them as Gaussian mixtures observed in real-world dataset experiments.
- **CUSUM Sinmix:** Assumes full knowledge of  $f_\phi$  but only partial knowledge of  $g_\theta$ , using Gaussian estimation to approximate the post-change distribution.
- **CUSUM Single:** Assumes partial knowledge of both  $f_\phi$  and  $g_\theta$ , modeling each as a single Gaussian distribution.

## 6.2 Numerical Results

To assess the performance of our CUSUM-based change detection approach, we employ the methodology described in Section 5.2. Below, we present numerical results that measure the expectation values across varying levels of distributional knowledge. As illustrated in Table 7, each knowledge level corresponds to a distinct algorithmic implementation. The expectation value varies depending on the integration base: for  $t < \gamma$ , we integrate with respect to  $f_\phi$ , whereas for  $t \geq \gamma$ , we use  $g_\theta$  as the base.

Table 7. Representation of expectation values for corresponding algorithms under varying levels of distribution knowledge.

Distribution	Algorithm	$\mathbb{E}_{t < \gamma}[\log \hat{L}(\epsilon)]$	$\mathbb{E}_{t \geq \gamma}[\log \hat{L}(\epsilon)]$
Complete	CUSUM Mix	$-D_{KL}(f_\phi \  g_\theta)$	$D_{KL}(g_\theta \  f_\phi)$
Partial Post	CUSUM Sinmix	$-D_{KL}(f_\phi \  \hat{g}_\theta)$	$D_{KL}(g_\theta(\epsilon) \  f_\phi(\epsilon)) - D_{KL}(g_\theta(\epsilon) \  \hat{g}_\theta(\epsilon))$
Partial Pre & Post	CUSUM Single	$-D_{KL}(f_\phi \  \hat{g}_\theta) + D_{KL}(f_\phi \  \hat{f}_\phi)$	$D_{KL}(g_\theta \  \hat{f}_\phi) - D_{KL}(g_\theta \  \hat{g}_\theta)$

**Expectation.** The numerical evaluation of CUSUM-based change detection under varying distributional knowledge levels (Table 8) demonstrates alignment with theoretical requirements: pre-change expectations  $\mathbb{E}_{t < \gamma}[\log \hat{L}(\epsilon)]$  are strictly negative across all algorithms (*e.g.*, CUSUM Mix:  $-1.90$  ADE for FQA), satisfying the false alarm suppression criterion, while post-change expectations  $\mathbb{E}_{t \geq \gamma}[\log \hat{L}(\epsilon)]$  remain positive (*e.g.*, CUSUM Mix:  $1.98$  ADE for GRIP++), ensuring detection reliability. The results validate the theoretical expressions derived from KL divergences—complete knowledge (CUSUM Mix) achieves maximal post-change detectability ( $D_{KL}(g_\theta \| f_\phi)$ ) but incurs higher pre-change penalties ( $-D_{KL}(f_\phi \| g_\theta)$ ), whereas partial knowledge methods (CUSUM Sinmix/Single) exhibit lower expectation values (*e.g.*, CUSUM Sinmix post-change expectation  $< 1.09$  and CUSUM Single post-change expectation  $< 0.71$ ).

**Variance and Stability.** The variance analysis (Table 9) reveals distinct stability patterns across groups. CUSUM Mix/Sinmix shows moderate to high variances: CUSUM Mix maintains stable pre-change variances ( $\sigma^2 \approx 0.40$ – $0.43$ ), slightly decreasing post-change ( $\sigma^2 \approx 0.36$ – $0.40$ ), while CUSUM Sinmix exhibits higher pre-change ( $\sigma^2 \approx 0.45$ – $0.54$ ) and sharply rising post-change variances ( $\sigma^2 \approx 0.75$ – $0.88$ ), reflecting approximation challenges, which may also stem from inherent randomness. CUSUM Single demonstrates exceptional stability, with pre-change variances  $\sigma^2 \leq 0.07$  and



Table 8. Numerical evaluation of  $\mathbb{E}_{t < \gamma}[\log \hat{L}(\epsilon)]$  and  $\mathbb{E}_{t \geq \gamma}[\log \hat{L}(\epsilon)]$  across GRIP++ and FQA model and three metrics (ApolloScape dataset). The outstanding result is emphasized in bold.

Algo	GRIP++			FQA			Algo	GRIP++			FQA		
	ADE	FDE	RMSE	ADE	FDE	RMSE		ADE	FDE	RMSE	ADE	FDE	RMSE
★ Mix	-1.69	-1.77	-1.73	<b>-1.90</b>	-1.28	-2.14	★ Mix	<b>1.98</b>	1.44	1.75	1.01	1.17	1.75
★ Sinmix	-1.08	<b>-1.39</b>	-0.98	-0.99	-0.84	-0.94	★ Sinmix	0.95	0.85	0.98	0.85	<b>1.09</b>	0.92
★ Single	-0.72	<b>-1.12</b>	-0.70	-0.63	-0.77	-1.02	★ Single	0.54	0.62	0.70	0.51	0.66	<b>0.71</b>

(a) Expected value of pre-change ( $t < \gamma$ )

(b) Expected value of post-change ( $t \geq \gamma$ )

Represent CUSUM using the symbol ★ (due to space constraints).

Table 9. Variance of  $\mathbb{E}_{t < \gamma}[\log \hat{L}(\epsilon)]$  and  $\mathbb{E}_{t \geq \gamma}[\log \hat{L}(\epsilon)]$  across GRIP++ and FQA model and three metrics (ApolloScape dataset). The outstanding result is emphasized in bold.

Algo	GRIP++			FQA			Algo	GRIP++			FQA		
	ADE	FDE	RMSE	ADE	FDE	RMSE		ADE	FDE	RMSE	ADE	FDE	RMSE
★ Mix	<b>0.40</b>	0.42	0.41	0.43	0.42	0.41	★ Mix	0.38	0.39	0.37	<b>0.36</b>	0.40	0.36
★ Sinmix	0.47	<b>0.45</b>	0.46	0.53	0.52	0.54	★ Sinmix	0.88	0.88	0.81	0.76	<b>0.75</b>	0.76
★ Single	0.05	<b>0.04</b>	0.06	0.06	0.05	0.07	★ Single	0.06	<b>0.04</b>	<b>0.04</b>	0.05	0.05	0.06

(a) Pre-change Variance ( $\sigma^2$ ) ( $t < \gamma$ )

(b) Post-change Variance ( $\sigma^2$ ) ( $t \geq \gamma$ )

post-change  $\sigma^2 \leq 0.06$ , validating its robustness under the same distributional assumption (*i.e.*, single Gaussian). These trends highlight the trade-off between knowledge granularity and stability, offering valuable insights into maintaining practical reliability even in the face of increased approximation uncertainty.

### 6.3 CUSUM Change-point Detection

**CUSUM Detection of ID and OOD Scene.** Fig. 8 illustrates the effectiveness of the CUSUM algorithm in detecting abnormal shifts in AV’s trajectory prediction by tracking changes in prediction errors. The detection relies on monitoring the cumulative statistic  $W_t$ , which sums the log-likelihood ratios between pre-change and post-change distributions. A change is declared when  $W_t$  exceeds a predefined threshold  $b$ . In the OOD scene (Fig. 8a), a perturbation is introduced at time step 490, and we observe that  $W_t$  rapidly increases, crossing the threshold  $b = 7$  at time step 504. This triggers a detection with a delay of only 14 samples. In contrast, in the ID scene (Fig. 8b), prediction errors remain stable, and  $W_t$  never exceeds the threshold  $b$ . Consequently, no change point is detected, confirming that the vehicle’s trajectory aligns with typical patterns and that no false alarm is raised.

**Worst-case Average Detection Delay.** To evaluate detection delay across algorithms, all methods were standardized to identical MTFA conditions, as illustrated in Fig. 9. Detection thresholds were systematically calibrated for each algorithm to achieve parity in MTFA performance. For rigorous statistical validation, experiments were conducted with a predefined change point at time step 0 to measure worst-case average detection delay (WADD), with 10,000 independent trials performed per method. Results revealed significant performance disparities: CUSUM Mix exhibited the shortest detection delay at 3 samples, outperforming CUSUM Sinmix (5 samples) and CUSUM Single (8 samples). In contrast, the Z-Score method required 15 samples for detection, while the baseline Chi-Square method lagged substantially at

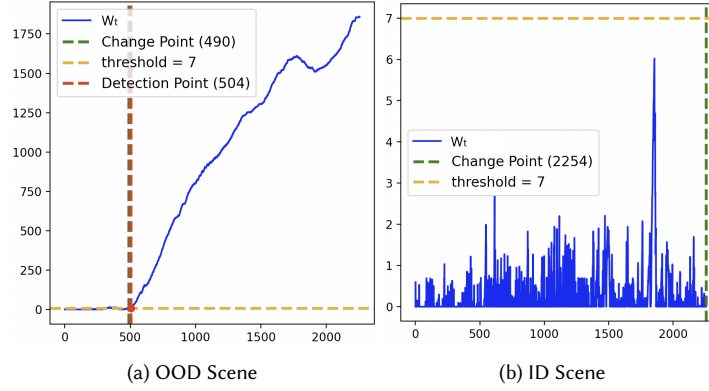


Fig. 8. Statistical evolution of CUSUM detection given the prediction errors from both ID and OOD scenes. A change occurs at step 490, i.e.,  $\gamma = 490$ . The threshold  $b$  is chosen to be 7. At time step 504, the statistic  $W_t$  surpasses the threshold ( $b = 7$ ), declaring the detection of a change. The detection delay is 14 time steps. This illustrating experiment is conducted using the GRIP++ model on the ApolloScape dataset, with prediction errors evaluated using the ADE metric.

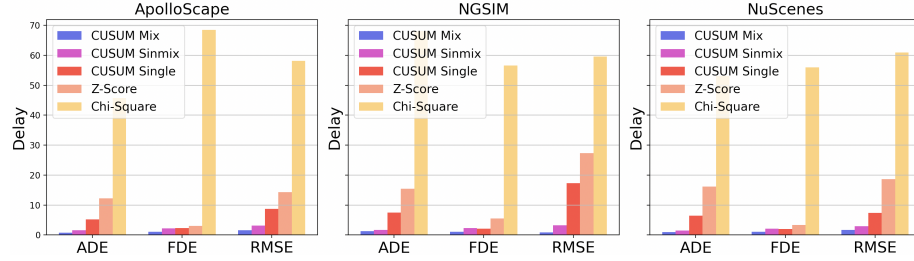


Fig. 9. WADD of the tested OOD detection algorithms across different metrics under the same MTFA. The delay is measured using **ADE**, **FDE**, and **RMSE**, providing a comparative analysis of algorithm performance in identifying anomalies. Lower delay values indicate faster detection. GRIP++ Model is used for illustration.

50 samples on the ApolloScape dataset using the ADE metric. This comparative analysis underscores the superior responsiveness of CUSUM-based approaches in time-sensitive change detection scenarios, highlighting their practical advantage in applications demanding rapid anomaly identification with controlled false-alarm rates.

**False Alarm-Delay Trade-off Analysis.** We further evaluate detection reliability across varying MTFA constraints. Fig. 10 presents a comparative evaluation of Algorithm 1 applied to benchmark models GRIP++ and FQA across three datasets and three performance metrics. Across all experiments, CUSUM Mix demonstrates the most favorable trade-off, achieving the lowest detection delay while maintaining a comparable MTFA to other algorithms. CUSUM Sinmix and CUSUM Single follow, though their performance declines due to limited distributional knowledge. Nevertheless, cross-dataset validation (thumbnail in Fig. 10) confirms the robustness of CUSUM-based methods. Their predictable delay scaling under dynamic thresholds—unlike the erratic behavior of Z-Score and Chi-Square—positions them as preferred solutions for real-time systems requiring simultaneous precision and responsiveness. This stability is particularly critical in applications where false-alarm constraints evolve dynamically, such as autonomous navigation or industrial monitoring.

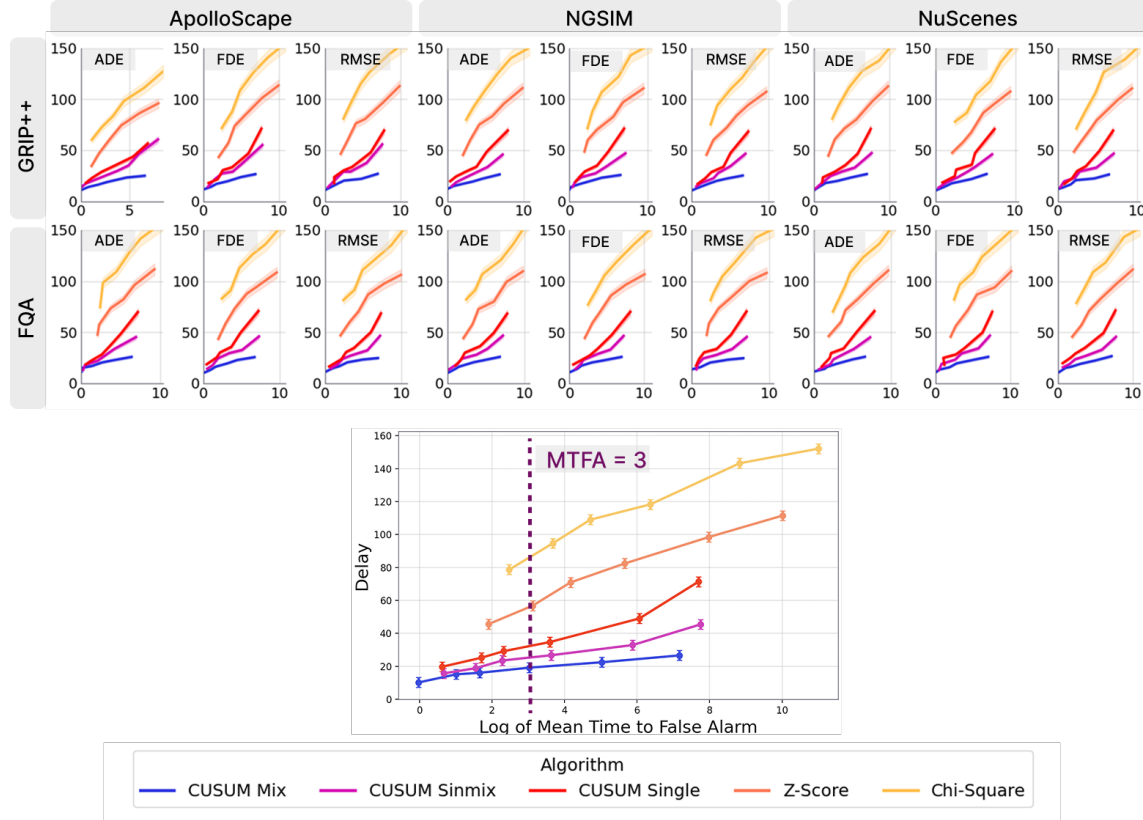


Fig. 10. Performance of Delay over MTFA, shown for both thumbnail (overview) and zoomed-in image (detailed view). **Thumbnail (overview)** compares GRIP++ (top row) and FQA (bottom row). Each row is organized in groups of three: the first three columns correspond to the ApolloScape datasets, followed by NGSIM and NuScenes. Within each group, the metrics are arranged as ADE, FDE, and RMSE, highlighting trends and ensuring consistent performance across various scenarios. **Single image (detailed view)** presents an example using the GRIP++ model and the ADE metric, with the threshold  $b$  increasing from left to right.

## 7 CONCLUSION

We propose lightweight Quick Change Detection (QCD) methods for detecting out-of-distribution (OOD) scenes in real-world trajectory prediction datasets, introducing a novel approach in this field. Our method monitors a scalar variable of prediction errors, enabling OOD detection at any point during inference. Unlike prior studies that rely heavily on simulated environments, we rigorously address this challenge using three real-world datasets—ApolloScape, NGSIM, and NuScenes—alongside two state-of-the-art prediction models, GRIP++ and FQA. Our work demonstrates the feasibility and effectiveness of applying CUSUM-based algorithms for timely and accurate OOD detection in AV systems. Experimental results show that CUSUM Mix consistently achieves superior detection performance with minimal false alarms, particularly when modeled using GMMs across all dataset-model combinations. These findings provide a robust solution for enhancing the safety and reliability of AV systems through timely model adjustments in dynamic environments.

For future work, first, we plan to explore the development of a tiered alarm system with multiple thresholds, enabling context-aware alerts that prioritize critical warnings while filtering out benign anomalies. Such an approach could reduce computational overhead and enhance operational efficiency. Moreover, we want to further propose the adaptation solutions after the OOD scene is detected. We will explore imitation-based techniques to refine the system's ability to mimic expert decision-making in OOD scenes. By leveraging imitation learning, the system can learn from human or expert interventions during rare or critical events, improving its ability to generalize to unseen situations. This will involve training the model on annotated datasets where expert responses to OOD events are recorded, enabling the system to better predict and respond to similar anomalies in real-time.

## REFERENCES

- [1] Cyrus Anderson, Ram Vasudevan, and Matthew Johnson-Roberson. 2021. A kinematic model for trajectory prediction in general highway scenarios. *IEEE Robotics and Automation Letters* 6, 4 (2021), 6757–6764.
- [2] Taposh Banerjee and Venugopal V Veeravalli. 2015. Data-efficient quickest change detection in sensor networks. *IEEE Transactions on Signal Processing* 63, 14 (2015), 3727–3735.
- [3] Holger Caesar, Varun Bankiti, Alex H Lang, Sourabh Vora, Venice Erin Liong, Qiang Xu, Anush Krishnan, Yu Pan, Giancarlo Baldan, and Oscar Beijbom. 2020. nuscenes: A multimodal dataset for autonomous driving. In *Proceedings of the IEEE/CVF conference on computer vision and pattern recognition*. nill, nill, 11621–11631.
- [4] Chris Cheadle, Marquis P Vawter, William J Freed, and Kevin G Becker. 2003. Analysis of microarray data using Z score transformation. *The Journal of molecular diagnostics* 5, 2 (2003), 73–81.
- [5] Sharon Chiang, John Zito, Vikram R Rao, and Marina Vannucci. 2024. Time-Series Analysis. In *Statistical Methods in Epilepsy*. Chapman and Hall/CRC, nill, 166–200.
- [6] Seongjin Choi, Jiwon Kim, and Hwasoo Yeo. 2021. TrajGAIL: Generating urban vehicle trajectories using generative adversarial imitation learning. *Transportation Research Part C: Emerging Technologies* 128 (2021), 103091.
- [7] Md Foezur Rahman Chowdhury, S-A Selouani, and D O'Shaughnessy. 2012. Bayesian on-line spectral change point detection: a soft computing approach for on-line ASR. *International Journal of Speech Technology* 15 (2012), 5–23.
- [8] Henggang Cui, Vladan Radosavljevic, Fang-Chieh Chou, Tsung-Han Lin, Thi Nguyen, Tzu-Kuo Huang, Jeff Schneider, and Nemanja Djuric. 2019. Multimodal trajectory predictions for autonomous driving using deep convolutional networks. In *2019 international conference on robotics and automation (icra)*. IEEE, nill, nill, 2090–2096.
- [9] Patrick Dendorfer, Sven Elflein, and Laura Leal-Taixé. 2021. Mg-gan: A multi-generator model preventing out-of-distribution samples in pedestrian trajectory prediction. In *Proceedings of the IEEE/CVF International Conference on Computer Vision*. nill, nill, 13158–13167.
- [10] Nachiket Deo, Akshay Rangesh, and Mohan M Trivedi. 2018. How would surround vehicles move? A unified framework for maneuver classification and motion prediction. *IEEE Transactions on Intelligent Vehicles* 3, 2 (2018), 129–140.
- [11] Nachiket Deo and Mohan M Trivedi. 2018. Convolutional social pooling for vehicle trajectory prediction. In *Proceedings of the IEEE conference on computer vision and pattern recognition workshops*. nill, nill, 1468–1476.
- [12] Zhen Fang, Yixuan Li, Jie Lu, Jiahua Dong, Bo Han, and Feng Liu. 2022. Is out-of-distribution detection learnable? *Advances in Neural Information Processing Systems* 35 (2022), 37199–37213.
- [13] Federal Highway Administration. 2020. *Traffic Analysis Tools: Next Generation Simulation*. nill. <https://ops.fhwa.dot.gov/trafficanalysistools/ngsim.htm> [Accessed: Sep. 13, 2024].
- [14] Angelos Filos, Panagiotis Tigkas, Rowan McAllister, Nicholas Rhinehart, Sergey Levine, and Yarin Gal. 2020. Can autonomous vehicles identify, recover from, and adapt to distribution shifts?. In *International Conference on Machine Learning*. PMLR, nill, nill, 3145–3153.
- [15] Todd Michael Franke, Timothy Ho, and Christina A Christie. 2012. The chi-square test: Often used and more often misinterpreted. *American journal of evaluation* 33, 3 (2012), 448–458.

- [16] David Sierra González, Jilles Steeve Dibangoye, and Christian Laugier. 2016. High-speed highway scene prediction based on driver models learned from demonstrations. In *2016 IEEE 19th International Conference on Intelligent Transportation Systems (ITSC)*. IEEE, nill, nill, 149–155.
- [17] Jie Guo, Hao Yan, and Chen Zhang. 2023. A Bayesian partially observable online change detection approach with Thompson sampling. *Technometrics* 65, 2 (2023), 179–191.
- [18] Dan Hendrycks and Kevin Gimpel. 2016. A baseline for detecting misclassified and out-of-distribution examples in neural networks. *arXiv preprint arXiv:1610.02136* nill, nill (2016), nill.
- [19] Yingze Hou, Hoda Bidkhori, and Taposh Banerjee. 2024. Robust Quickest Change Detection in Multi-Stream Non-Stationary Processes. *arXiv preprint arXiv:2412.04493* nill, nill (2024), nill.
- [20] Xinyu Huang, Xinjing Cheng, Qichuan Geng, Binbin Cao, Dingfu Zhou, Peng Wang, Yuanqing Lin, and Ruigang Yang. 2018. The apolloscape dataset for autonomous driving. In *Proceedings of the IEEE conference on computer vision and pattern recognition workshops*. nill, nill, 954–960.
- [21] Xin Huang, Stephen G. McGill, Brian C. Williams, Luke Fletcher, and Guy Rosman. 2019. Uncertainty-Aware Driver Trajectory Prediction at Urban Intersections. In *2019 International Conference on Robotics and Automation (ICRA)*. nill, nill, 9718–9724. <https://doi.org/10.1109/ICRA.2019.8794282>
- [22] Naoki Itoh and Jürgen Kurths. 2010. Change-point detection of climate time series by nonparametric method. In *Proceedings of the world congress on engineering and computer science*, Vol. 1. nill, nill, 445–448.
- [23] Boris Ivanovic and Marco Pavone. 2022. Injecting planning-awareness into prediction and detection evaluation. In *2022 IEEE Intelligent Vehicles Symposium (IV)*. IEEE, nill, nill, 821–828.
- [24] Ashesh Jain, Amir R Zamir, Silvio Savarese, and Ashutosh Saxena. 2016. Structural-rnn: Deep learning on spatio-temporal graphs. In *Proceedings of the IEEE conference on computer vision and pattern recognition*. nill, nill, 5308–5317.
- [25] Nico Kaempchen, Bruno Schiele, and Klaus Dietmayer. 2009. Situation assessment of an autonomous emergency brake for arbitrary vehicle-to-vehicle collision scenarios. *IEEE Transactions on Intelligent Transportation Systems* 10, 4 (2009), 678–687.
- [26] Nitin Kamra, Hao Zhu, Dweep Kumarbhai Trivedi, Ming Zhang, and Yan Liu. 2020. Multi-agent trajectory prediction with fuzzy query attention. *Advances in Neural Information Processing Systems* 33 (2020), 22530–22541.
- [27] Hayoung Kim, Dongchan Kim, Gihoon Kim, Jeongmin Cho, and Kunsoo Huh. 2020. Multi-head attention based probabilistic vehicle trajectory prediction. In *2020 IEEE Intelligent Vehicles Symposium (IV)*. IEEE, nill, nill, 1720–1725.
- [28] Lifeng Lai, Yijia Fan, and H Vincent Poor. 2008. Quickest detection in cognitive radio: A sequential change detection framework. In *IEEE GLOBECOM 2008-2008 IEEE Global Telecommunications Conference*. IEEE, nill, nill, 1–5.
- [29] Tze Siong Lau, Wee Peng Tay, and Venugopal V Veeravalli. 2018. A binning approach to quickest change detection with unknown post-change distribution. *IEEE Transactions on Signal Processing* 67, 3 (2018), 609–621.
- [30] Kimin Lee, Kibok Lee, Honglak Lee, and Jinwoo Shin. 2018. A simple unified framework for detecting out-of-distribution samples and adversarial attacks. *Advances in neural information processing systems* 31, nill (2018), nill.
- [31] Namhoon Lee, Wongun Choi, Paul Vernaza, Christopher B Choy, Philip HS Torr, and Manmohan Chandraker. 2017. Desire: Distant future prediction in dynamic scenes with interacting agents. In *Proceedings of the IEEE conference on computer vision and pattern recognition*. nill, nill, 336–345.
- [32] Jingyao Li, Pengguang Chen, Zexin He, Shaozuo Yu, Shu Liu, and Jiaya Jia. 2023. Rethinking out-of-distribution (ood) detection: Masked image modeling is all you need. In *Proceedings of the IEEE/CVF conference on computer vision and pattern recognition*. nill, nill, 11578–11589.
- [33] Kaican Li, Kai Chen, Haoyu Wang, Lanqing Hong, Chaoqiang Ye, Jianhua Han, Yukuai Chen, Wei Zhang, Chunjing Xu, Dit-Yan Yeung, et al. 2022. Coda: A real-world road corner case dataset for object detection in autonomous driving. In *European Conference on Computer Vision*. Springer, nill, nill, 406–423.
- [34] Xin Li, Xiaowen Ying, and Mooi Choo Chuah. 2019. Grip++: Enhanced graph-based interaction-aware trajectory prediction for autonomous driving. *arXiv preprint arXiv:1907.07792* nill, nill (2019), nill.

- [35] Yang Li, Xiao-Yun Lu, Jianqiang Wang, and Keqiang Li. 2020. Pedestrian trajectory prediction combining probabilistic reasoning and sequence learning. *IEEE transactions on intelligent vehicles* 5, 3 (2020), 461–474.
- [36] Yuchen Liang and Venugopal V Veeravalli. 2024. Quickest Change Detection with Post-Change Density Estimation. *IEEE Transactions on Information Theory* nill, nill (2024), nill.
- [37] Chiu-Feng Lin, A Galip Ulsoy, and David J LeBlanc. 2000. Vehicle dynamics and external disturbance estimation for vehicle path prediction. *IEEE Transactions on Control Systems Technology* 8, 3 (2000), 508–518.
- [38] Mengmeng Liu, Hao Cheng, Lin Chen, Hellward Broszio, Jiangtao Li, Runjiang Zhao, Monika Sester, and Michael Ying Yang. 2024. Laformer: Trajectory prediction for autonomous driving with lane-aware scene constraints. In *Proceedings of the IEEE/CVF Conference on Computer Vision and Pattern Recognition*. nill, nill, 2039–2049.
- [39] Weitang Liu, Xiaoyun Wang, John Owens, and Yixuan Li. 2020. Energy-based out-of-distribution detection. *Advances in neural information processing systems* 33 (2020), 21464–21475.
- [40] Gary Lorden. 1971. Procedures for reacting to a change in distribution. *The annals of mathematical statistics* nill, nill (1971), 1897–1908.
- [41] Panagiotis Lytrivis, George Thomaidis, and Angelos Amditis. 2008. Cooperative path prediction in vehicular environments. In *2008 11th international IEEE conference on intelligent transportation systems*. IEEE, nill, nill, 803–808.
- [42] Rakesh Malladi, Giridhar P Kalamangalam, and Behnaam Aazhang. 2013. Online Bayesian change point detection algorithms for segmentation of epileptic activity. In *2013 Asilomar conference on signals, systems and computers*. IEEE, nill, nill, 1833–1837.
- [43] Gunasekaran Manogaran and Daphne Lopez. 2018. Spatial cumulative sum algorithm with big data analytics for climate change detection. *Computers & Electrical Engineering* 65 (2018), 207–221.
- [44] Davide Salvatore Mare, Fernando Moreira, and Roberto Rossi. 2017. Nonstationary Z-score measures. *European Journal of Operational Research* 260, 1 (2017), 348–358.
- [45] Murad Mebrahtu, Awet Araia, Abiel Ghebreslasie, Jorge Dias, and Majid Khonji. 2023. Transformer-Based Multi-Modal Probabilistic Pedestrian Prediction for Risk-Aware Autonomous Vehicle Navigation. In *2023 21st International Conference on Advanced Robotics (ICAR)*. IEEE, nill, nill, 652–659.
- [46] Timothy L Molloy and Jason J Ford. 2017. Misspecified and asymptotically minimax robust quickest change detection. *IEEE Transactions on Signal Processing* 65, 21 (2017), 5730–5742.
- [47] George V Moustakides. 1986. Optimal stopping times for detecting changes in distributions. *the Annals of Statistics* 14, 4 (1986), 1379–1387.
- [48] Igor V Nikiforov. 1995. A generalized change detection problem. *IEEE Transactions on Information theory* 41, 1 (1995), 171–187.
- [49] Ewan S Page. 1954. Continuous inspection schemes. *Biometrika* 41, 1/2 (1954), 100–115.
- [50] Muzi Peng, Jiangwei Wang, Dongjin Song, Fei Miao, and Lili Su. 2023. Privacy-Preserving and Uncertainty-Aware Federated Trajectory Prediction for Connected Autonomous Vehicles. In *2023 IEEE/RSJ International Conference on Intelligent Robots and Systems (IROS)*. IEEE, nill, nill, 11141–11147.
- [51] Romain Pepy, Alain Lambert, and Hugues Mounier. 2006. Reducing navigation errors by planning with realistic vehicle model. In *2006 IEEE Intelligent Vehicles Symposium*. IEEE, nill, nill, 300–307.
- [52] Tung Phan-Minh, Elena Corina Grigore, Freddy A Boulton, Oscar Beijbom, and Eric M Wolff. 2020. Covernet: Multimodal behavior prediction using trajectory sets. In *Proceedings of the IEEE/CVF conference on computer vision and pattern recognition*. nill, nill, 14074–14083.
- [53] Mengshi Qi, Jie Qin, Yu Wu, and Yi Yang. 2020. Imitative non-autoregressive modeling for trajectory forecasting and imputation. In *Proceedings of the IEEE/CVF Conference on Computer Vision and Pattern Recognition*. nill, nill, 12736–12745.
- [54] Rakesh Rana and Richa Singhal. 2015. Chi-square test and its application in hypothesis testing. *Journal of Primary Care Specialties* 1, 1 (2015), 69–71.
- [55] Jaxk Reeves, Jien Chen, Xiaolan L Wang, Robert Lund, and Qi Qi Lu. 2007. A review and comparison of changepoint detection techniques for climate data. *Journal of applied meteorology and climatology* 46, 6 (2007), 900–915.



- [56] Jie Ren, Stanislav Fort, Jeremiah Liu, Abhijit Guha Roy, Shreyas Padhy, and Balaji Lakshminarayanan. 2021. A simple fix to mahalanobis distance for improving near-ood detection. *arXiv preprint arXiv:2106.09022* nill, nill (2021), nill.
- [57] Macheng Shen, Golnaz Habibi, and Jonathan P How. 2018. Transferable pedestrian motion prediction models at intersections. In *2018 IEEE/RSJ International Conference on Intelligent Robots and Systems (IROS)*. nill, nill, nill, 4547–4553.
- [58] Albert N Shiryaev. 1963. On optimum methods in quickest detection problems. *Theory of Probability & Its Applications* 8, 1 (1963), 22–46.
- [59] Li Song, Ruijia Wang, Ding Xiao, Xiaotian Han, Yanan Cai, and Chuan Shi. 2018. Anomalous trajectory detection using recurrent neural network. In *Advanced Data Mining and Applications: 14th International Conference, ADMA 2018, Nanjing, China, November 16–18, 2018, Proceedings 14*. Springer, nill, nill, 263–277.
- [60] Yiyu Sun, Yifei Ming, Xiaojin Zhu, and Yixuan Li. 2022. Out-of-distribution detection with deep nearest neighbors. In *International Conference on Machine Learning*. PMLR, nill, nill, 20827–20840.
- [61] Zhongchang Sun, Shaofeng Zou, Ruizhi Zhang, and Qunwei Li. 2022. Quickest change detection in anonymous heterogeneous sensor networks. *IEEE Transactions on Signal Processing* 70 (2022), 1041–1055.
- [62] Fahim Tajwar, Ananya Kumar, Sang Michael Xie, and Percy Liang. 2021. No true state-of-the-art? ood detection methods are inconsistent across datasets. *arXiv preprint arXiv:2109.05554* nill, nill (2021), nill.
- [63] Xiaolin Tang, Tong Jia, Xiaosong Hu, Yanjun Huang, Zhongwei Deng, and Huayan Pu. 2020. Naturalistic data-driven predictive energy management for plug-in hybrid electric vehicles. *IEEE Transactions on Transportation Electrification* 7, 2 (2020), 497–508.
- [64] Xiaolong Tang, Meina Kan, Shiguang Shan, Zhilong Ji, Jinfeng Bai, and Xilin Chen. 2024. Hpnet: Dynamic trajectory forecasting with historical prediction attention. In *Proceedings of the IEEE/CVF Conference on Computer Vision and Pattern Recognition*. nill, nill, 15261–15270.
- [65] Xiaolin Tang, Kai Yang, Hong Wang, Jiahang Wu, Yechen Qin, Wenhao Yu, and Dongpu Cao. 2022. Prediction-Uncertainty-Aware Decision-Making for Autonomous Vehicles. *IEEE Transactions on Intelligent Vehicles* 7, 4 (2022), 849–862. <https://doi.org/10.1109/TIV.2022.3188662>
- [66] Alexander Tartakovsky, Igor Nikiforov, and Michele Basseville. 2014. *Sequential analysis: Hypothesis testing and changepoint detection*. CRC press, nill.
- [67] Alexander G Tartakovsky, Aleksey S Polunchenko, and Grigory Sokolov. 2012. Efficient computer network anomaly detection by changepoint detection methods. *IEEE Journal of Selected Topics in Signal Processing* 7, 1 (2012), 4–11.
- [68] Alexander G Tartakovsky, Boris L Rozovskii, Rudolf B Blažek, and Hongjoong Kim. 2006. Detection of intrusions in information systems by sequential change-point methods. *Statistical methodology* 3, 3 (2006), 252–293.
- [69] Alexander G Tartakovsky and Venugopal V Veeravalli. 2005. General asymptotic Bayesian theory of quickest change detection. *Theory of Probability & Its Applications* 49, 3 (2005), 458–497.
- [70] Franco van Wyk, Yiyang Wang, Anahita Khojandi, and Neda Masoud. 2020. Real-Time Sensor Anomaly Detection and Identification in Automated Vehicles. *IEEE Transactions on Intelligent Transportation Systems* 21, 3 (2020), 1264–1276. <https://doi.org/10.1109/TITS.2019.2906038>
- [71] Venugopal V Veeravalli and Taposh Banerjee. 2014. Quickest change detection. In *Academic press library in signal processing*. Vol. 3. Elsevier, nill, 209–255.
- [72] W Allen Wallis and Geoffrey H Moore. 1941. A significance test for time series analysis. *J. Amer. Statist. Assoc.* 36, 215 (1941), 401–409.
- [73] Chujie Wang, Lin Ma, Rongpeng Li, Tariq S Durrani, and Honggang Zhang. 2019. Exploring trajectory prediction through machine learning methods. *IEEE Access* 7 (2019), 101441–101452.
- [74] Jack M Wang, David J Fleet, and Aaron Hertzmann. 2007. Gaussian process dynamical models for human motion. *IEEE transactions on pattern analysis and machine intelligence* 30, 2 (2007), 283–298.
- [75] Ping Yang, Guy Dumont, and John Mark Ansermino. 2006. Adaptive change detection in heart rate trend monitoring in anesthetized children. *IEEE transactions on biomedical engineering* 53, 11 (2006), 2211–2219.

- [76] Qingzhao Zhang, Shengtuo Hu, Jiachen Sun, Qi Alfred Chen, and Z Morley Mao. 2022. On adversarial robustness of trajectory prediction for autonomous vehicles. In *Proceedings of the IEEE/CVF Conference on Computer Vision and Pattern Recognition*. nill, nill, 15159–15168.